Behavior of Rotating Stall Cell in a High Specific-Speed Diagonal Flow Fan

Norimasa Shiomi*, W. X. Cai, A. Muraoka, K. Kaneko, T. Setoguchi
Department of Mechanical Engineering, Saga Univ. , 1, Honjo-machi, Saga-shi, Saga-ken, 840-8502, Japan

An experimental investigation was carried out to clarify unsteady flow fields with rotating stall cell, especially behavior of stall cell, in a high specific-speed diagonal flow fan. As its specific-speed is very high for a diagonal flow fan, its pressure-flow rate curve tends to indicate unstable characteristics caused by rotating stall similar to axial flow fan. Although for an axial flow fan many researchers have investigated such the flow field, for a diagonal flow fan little study has been done. In this study, velocity fields at rotor inlet in a high specific-speed diagonal flow fan were measured by use of a single slant hot-wire probe. These data were processed by using the "Double Phase-Locked Averaging" (DPLA) technique, i. e. phases of both the rotor blade and the stall cell were taken into account. The behaviors of stall cell at rotor inlet were visualized for the meridional, tangential and radial velocity.

Key Words : Turbomachinery, Rotating Stall, Stall Cell, Unsteady Flow, Fan

1. Introduction

A diagonal flow fan has some good features, relatively high efficiency, low noise level and wide operating range. For a high specific-speed diagonal flow fan, however, its pressure-flow rate curve tends to indicate an unstable characteristic with a positive gradient in low flow range similar to axial flow fan. It is well known that the rotating stall is the main cause to this unstable characteristic, and the flow field with rotating stall indicates remarkable unsteadiness due to partly reversed flow.

For axial turbomachines, many investigations have been done for the stall inception and the flow field with rotating stall cell. From these papers, it is shown that there are two types of stall inception in axial compressors. One is long-length-scale disturbance type reported by Garnier et al. (1991). Moore and Greitzer (1986) had reported this phenomenon with two-dimensional linearized stability analysis. Poensgen and Gallus (1996) measured these flow fields by phase-locking data acquisition techniques with the cell rotation. According to the two-dimensional numerical simulation of the long-length-scale full-span stall by Saxer-Felice et al. (1998), a strong vortex bubble forming ahead of the rotor makes low pressure region. The other is short-length-scale disturbance type reported by McDougall et al. (1990). In many case, this type of stall inception was accompanied by multiple part-span stall cells. Mathioudakis and Breugelmans (1985) had reported this multiple wave disturbance caused by part-span cells in the low-speed axial compressor. Inoue et al. measured these flow field with rotating stall cell by use of "Double phase-locked averaging" (DPLA) technique with both the rotor and cell rotation.

On the other hand, for diagonal flow fan there are very few studies on unsteady flow field under rotating stall condition. Recently, for a diagonal flow fan, Kaneko et al. (1993 ; 1995 ; 1997 ; 2000)

* Corresponding Author,
E-mail : siomi@me. saga-u.ac.jp
TEL : +81-952-28-8684; **FAX** : +81-952-28-8587
Department of Mechanical Engineering, Saga Univ., 1, Honjo-machi, Saga-shi, Saga-ken, 840-8502, Japan.
(Manuscript **Received** August 11, 2001; **Revised** October 16, 2001)

tried to measure the unsteady flow field in rotating stall region by use of hot wire and pressure probe. In these experimental studies, unsteady flow characteristics of the rotating stall cell in a high specific-speed diagonal flow fan were clarified to some extent, but the behavior of stall cell has not yet been fully understood.

Most of surveys for the internal flow field of turbomachines have been carried out using a phase-lock average method, because the flow field changes periodically with blade passing frequency. But when the flow field includes rotating stall cell, the stall cell propagates at different speed with rotor blade. Therefore it is impossible to clarify the behavior of stall cell by means of the ordinary phase-lock average method. For the long-length-scale full-span stall cell, the flow fields were measured by phase-locking data acquisition techniques with the only cell rotation (Poensgen and Gallus, 1996), because in this case blade geometry has a secondary effect for the cell structure. On the other hand, for the short-length-scale part-span stall cell, it is necessary to get the data synchronously with both the rotor blade and the cell rotation. Inoue et al. exhibited that it is possible to clarify the flow field with short-length-scale stall cell by using the DPLA technique (Inoue et al.).

For a high specific-speed diagonal flow fan in Saga University, it has already shown that the stall cell occurring in this fan is part-span cell, the number of cell is one, and its propagating speed is approximately 80 per-cent of rotor speed. It seems that its type of stall cell is similar to long-length-scale stall cell. However, this cell is the part-span cell and its propagating speed is very high as for long-length-scale stall cell. Therefore, the DPLA technique is adopted in order to process the data of the unsteady flow fields with rotating stall cell. In this study, the authors carried out an experimental investigation on the unsteady flow field with rotating stall. Velocity measurements were performed on three measurement lines at rotor inlet with hot-wire anemometer by use of slant hot wire probe. The data taken were processed with the DPLA technique. The time-dependent ensemble averages were taken for three velocity components, i. e. meridional velocity (Vm), tangential velocity (Vt) and radial velocity (Vr). And the behavior of stall cell was visualized for each velocity component.

2. Experimental Apparatus and Procedure

The schematic layout of the test fan is shown in Fig. 1. The rotor blade element was designed by use of a quasi three dimensional method based on the two-dimensional cascade data. Selection of stator blade element was carried out using two-dimensional cascade data of circular-arc blade. The rotor was manufactured precisely by NC milling machine to secure the geometry of the rotor.

Specific speed of this fan is approximately 1600 (rpm, m^3/min, m). Although this is a relatively high value for a diagonal flow fan, this value were chosen to compare the flow field with an axial compressor, for which the researches on unsteady flow in the rotating stall region have been actively done. Another specifications are listed in Table 1.

Flow surveys of velocity vectors were carried out the upstream of the rotor by using a single slanted hot-wire. The probe traverse lines are shown in Fig. 1, where the distance between rotor blade leading edge and traverse line are 5mm (RF1), 10mm (RF2) and 15mm (RF3), respectively. Span-wise measurement stations are 12 points for each measurement line. The axis of the hot-wire probe was rotated at interval of 36 deg for 10 orientations of the sensor.

In the experiment, rotor blade signal, rotating stall cell signal and velocity data from a single

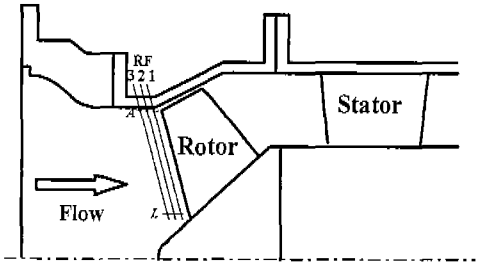

Fig. 1 Schematic layout of the test section

Table 1 Specifications of test fan, rotor and stator

Test Fan

Pressure coefficient	ψ=0.250
Flow coefficient	ϕ=0.345
Specific-speed	n_s=1620
Angle of casing	20
Angle of hub	40
Hub/tip ratio at stator	0.6

Rotor & Stator

	Rotor	Stator
Blade section	NACA 65	Circulararc
Number of blade	6	11
Mean solidity	0.88	1.30
Mean aspect ratio	0.79	0.67
Vortex design	Free vortex	Free vortex

slanted hot-wire probe were taken at the same time. Rotor blade signal is obtained from photo encoder. Rotating stall cell signal is obtained from the fast response pressure transducer through low pass filter (50Hz). The transducer is mounted on the outer casing wall and 5mm ahead from rotor leading edge. From each measurement station 450,000 data were sampled, whose sampling frequency was 20kHz. These data corresponded to approximately 1,200 revolutions of rotor and to 900 revolutions of stall cell. These data were processed by using the DPLA technique, i. e. the phases both rotor and stall cell were taken into account.

The test Reynolds number is about 3.1×10^5 based on the circumferential velocity and chord length of the rotor blade at mid-span section. Effect of tip clearance between rotor blade and outer casing on the stalling condition is remarkable. In this experiment it is selected to 0.5 mm.

3. Results and Discussions

3.1 Overall characteristics of test fan

The performance characteristics of the test fan are shown in Fig. 2, where abscissa indicates total pressure coefficient (ψ), efficiency (η), torque coefficient (τ) and ordinate represents flow rate

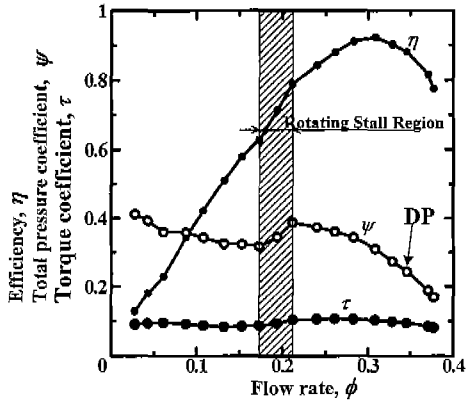

Fig. 2 Characteristic curves of test fan

(ϕ). When flow rate is reduced from design point (DP in Fig. 2), sharp drop in pressure coefficient occurs near ϕ=0.200. It was explained by Kaneko et al. (1993 ; 1995 ; 1997 ; 2001) that this sharp drop in pressure coefficient is due to occurrence of a rotating stall with one-cell and its propagating speed is approximately 80 percent of rotor speed. Internal flow measurements were conducted at this rotating stall condition (ϕ=0.195).

3.2 Meridional Velocity (Vm) Distributions at RF1 plane

Figures 3, 4 shows the contour maps of meridional velocity (Vm) distributions at RF1 under rotating stall condition with progressing Tp. Figure. 3 shows the full span pictures and Fig. 4 show the part span pictures near blade tip, from 82 percent of blade span to 95 percent. In all these figures, ordinate and abscissa indicate tangential direction (θ) and radial direction, respectively. Tp indicates the relative location of stall cell to rotor blade, and the rotating stall cell moves 1 pitch of the blade row from Tp=0.0 to 1.0. Therefore Tp is also considered to be non-dimensional time. There exist the regions enclosed by bold black line near outer casing. These lines indicate Vm=0.0. These are reversed flow region, and are correspond to stall cell. The value of Vm is normalized by rotor rotating speed at blade tip (Ut) and its maximum value of Vm/Ut is approximately 0.4. The interval between contour

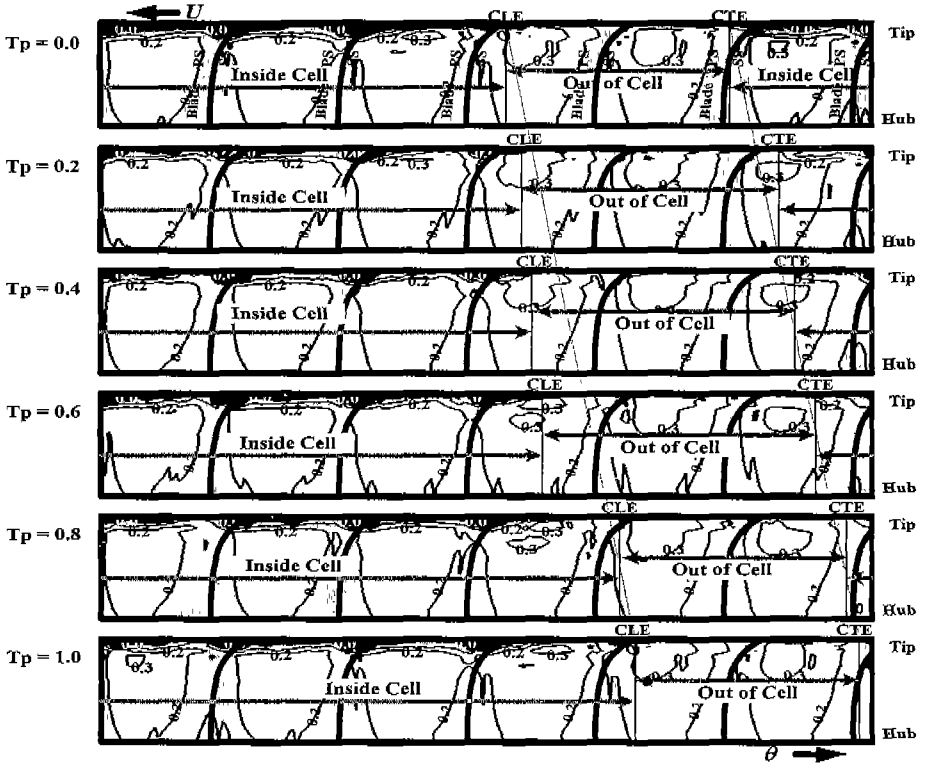

Fig. 3 Transition of meridional velocity (Vm) distributions with progressing Tp at RF1 (Full-span Pictures)

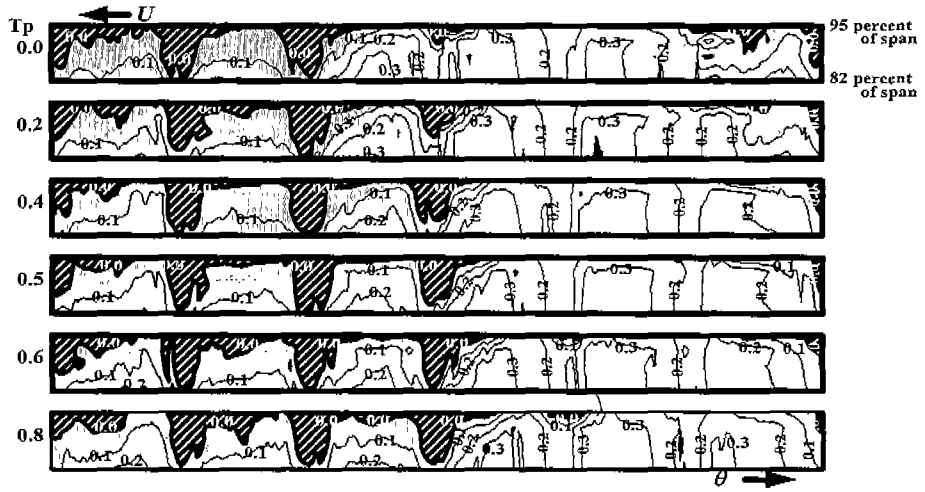

Fig. 4 Transition of meridional velocity distributions with progressing Tp at RF1 (Part-span pictures over 82 percent of rotor blade span)

lines in Fig. 3 and 4 is 0.1. The blade rotating direction (U) is shown at the top of the figure.

It is observed in Fig. 3 that the reversed flow region is limited near tip. Hence the cell in this fan is part-span cell. It is also seen that this region is moving from left to right in Fig. 3 with

progressing Tp. This propagating direction is opposite to the rotor blade motion (U). In this paper, hereafter, the right side edge of the cell is defined as the "cell leading edge" (CLE) and the left side as the "cell trailing edge" (CTE). Although the stall cell is moving at constant speed, the local speed at both edges is not constant. It is seemed that at CTE reversed flow region is gradually moving but at CLE it is suddenly jumping into next blade (see in Fig. 4, from Tp=0.5 to 0.6). This means that the circumferential size of the cell changes with progressing Tp. It is also observed that strong reversed flow exists on the blade pressure surface (PS) near blade tip. On the other hand, it is found that high meridional velocity regions exist out of the cell near tip. As the cell moves, under CLE these regions disappear with progressing Tp and under CTE it grows with progressing Tp.

As mentioned above, the flow fields with rotating stall cell and behaviour of stall cell are clarified in a high specific speed diagonal flow fan. The region of rotating stall cell in this fan extends widely toward tangential direction near outer casing. It is approximately 70 percent of a circumference. On the other hand, the radial depth is narrow. It is approximately 20 percent of blade span from outer casing. This is a feature of the stall cell in this fan. Its value is less than another results for axial compressors, presented by Poensgen and Gullus (1996), and Inoue et al. It is seemed that this is caused by the difference of the rotor geometry between an axial type and a diagonal type. In an axial type, the height of flow path on meridional plane is almost constant, but in a diagonal type it varies (see in Fig. 1).

For the distributions of Vm in this fan, it is observed that there are the periodical distributions of strongly reversed flow inside the cell, which are concentrated in near outer casing on blade PS. But in another results by Poensgen and Gullus (1996) or Inoue et al. such a periodical distribution is not observed. It is seemed that the reason is due to the difference of blade number. In our test fan, the number of rotor blade is only 6, while in Poensgen and Gullus (1996) it is 16 and in Inoue et al. it is 24. Therefore rotor blade spacing of our fan is wider than the rotor spacing of another case, and the effect of rotor blade spacing on the flow field is stronger than that of another case.

3.3 Tangential Velocity (Vt) Distributions at RF1 plane

Figure 5 shows the contour maps of tangential velocity (Vt) distributions with progressing Tp. In these figures, ordinate and abscissa indicate tangential direction (θ) and radial direction, respectively. The deep shadow regions parallel to outer casing near blade tip indicate the region with high value of Vt. In this case, the high value regions correspond to reversed flow regions in Fig. 3 and Fig. 4, i. e. this region is corresponding to the stall cell. The value of Vt is normalized by rotor rotating speed at blade tip (Ut) and its maximum value of Vt/Ut is approximately 0.8. This value is very high and it is approximately two times of Vm/Ut. The interval between contour lines in Fig. 5 is 0.1. The blade rotating direction is shown at the top of the figure.

In these figures the stall cell region is shown more clearly than the Vm distributions (Fig. 3 and 4). From these figures the regions with very high value of Vt/Ut is not blade PS but near blade suction surface (SS) at blade tip and extended to near centre of blade pitch. It means that when the blade is stalled, the separated flow on blade SS occurs, and its separated flow are moving with the blade. At clean flow region and under the cell (out of cell region), it is seen that the low velocity regions periodically exist. These indicate the effect of blade potential on flow field. In these figures, it is seemed that both CLE and CTE are gradually moving.

3.4 Radial Velocity (Vr) Distributions at RF1 plane

Figure 6 shows the contour maps of radial velocity (Vr) with progressing Tp. The radial velocity is normalized by rotor rotating speed at blade tip (Ut) and its maximum value of Vr/Ut is approximately 0.15. As this value is lower than Vm/Ut and Vt/Ut, it is seem that the effect of radial velocity on the flow field is not so large.

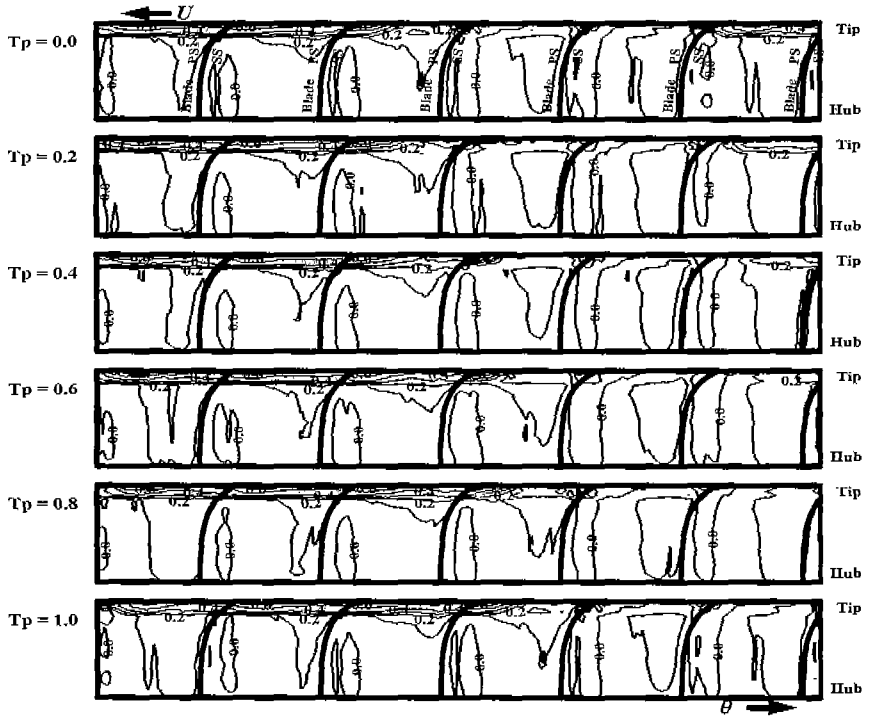

Fig. 5 Transition of tangential velocity distributions with progressing Tp at RF1

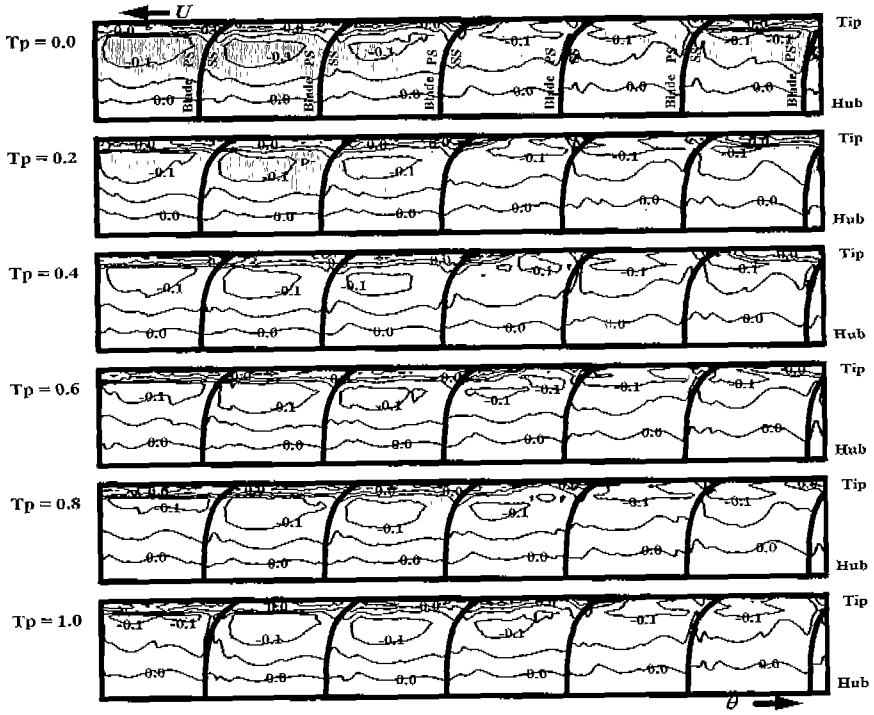

Fig. 6 Transition of radial velocity distributions with progressing Tp at RF1

The interval between contour lines in Fig. 6 is 0.05. The blade rotating direction (U) is shown at the top of the figure. It is noticed that the direction of radial velocity is parallel to the probe axis. Therefore when the flow comes in parallel to casing wall, its value becomes minus, on the other hand, parallel to hub its value is plus.

At the clean flow region (out of cell) near tip, the value of Vr/Ut shows minus, but as stated above, this means that inlet flow of this region is parallel to outer casing. Also, near hub the value of Vr/Ut shows plus, then the flow parallel to hub. Inside the cell, its value is mainly plus except for very near tip parts. This means that inside the cell the flow is mainly outwards.

3.5 Comparison for velocity distributions between different measurement planes

Figure 7, 8 shows the contour maps of meridional and tangential velocity distributions at three measurement planes at Tp=1.0, respectively. The top figure shows the Vm/Ut contour map at RF1, 5 mm upstream of rotor, the middle is at RF2, 10 mm upstream of rotor, and the bottom is at RF3, 15 mm upstream of rotor. These values are normalized by rotor rotating speed at blade tip (Ut). The blade rotating direction (U) is shown at the top of the figure.

It is found that the circumferential size of the stall cell becomes rapidly small in both figures as its distance becomes far from the rotor, but its radial size dose not change. It is also observed that the strength of reversed flow is almost same value for each measurement plane, but that the value of tangential velocity is rapidly weaken. At RF1 the maximum value of Vt/Ut is over 0.6, at RF2 it is approximately 0.4, and at RF3 it is approximately 0.2. As a result, it is found that the

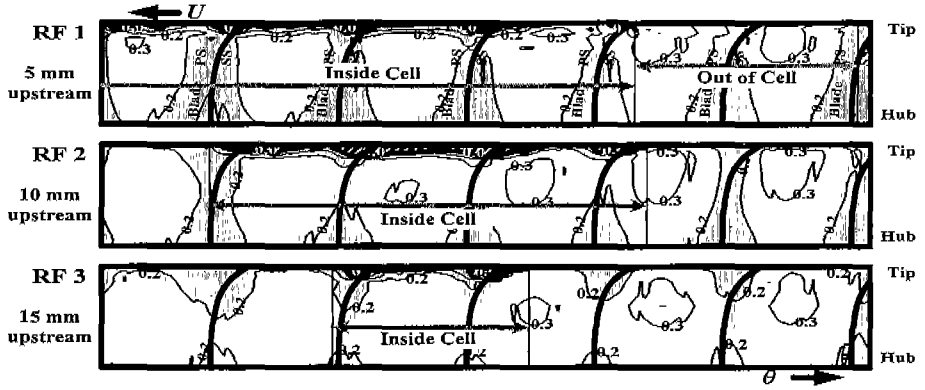

Fig. 7 Meridional velocity distributions on 3 measurement planes at rotor inlet with Tp=1.0

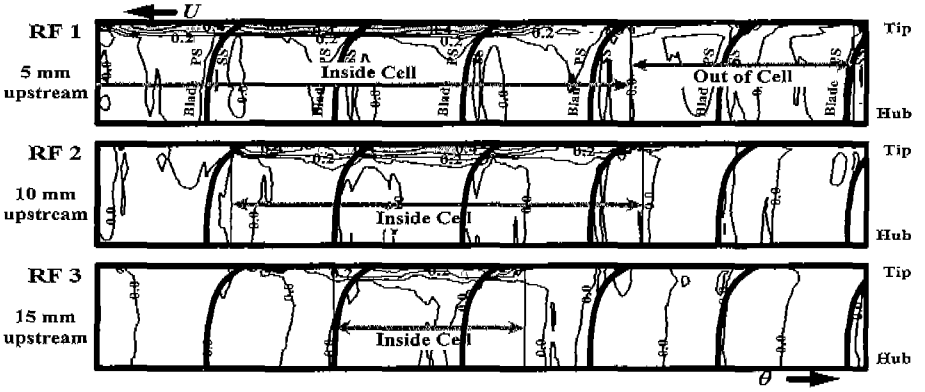

Fig. 8 Tangential velocity distributions on 3 measurement planes at rotor inlet with Tp=1.0

effect of the stall cell on rotor inlet flow field is generally weaken as its distance is far from the plane of rotor leading edge.

4. Conclusions

The unsteady flow fields at rotor inlet with rotating stall cell in a high specific-speed diagonal flow fan were clarified. To get these pictures, the measurements with a single slant hot-wire probe were conducted and these data were processed by use of double-phase-locked averaging technique. The main conclusions are obtained as follows.

(1) The stall cell in this fan is part-span cell. Its tangential size is approximately 70 percent of circumference, and its radial depth from outer casing is 20 percent of rotor blade span.

(2) There exist some periodical distributions of strongly reversed flow inside the cell.

(3) For meridional velocity, the strong reversed flow regions exist on blade PS near the blade tip in the cell. On the other hand, the sound main flow regions exist out of cell near outer casing. When the cell is propagating, it is gradually disappearing at CLE and it is gradually appearing at CTE.

(4) For tangential velocity, high tangential velocity regions exist blade SS at casing wall region.

(5) For radial velocity, the flow inside the stall cell is mainly outwards.

(6) The effect of the stall cell on rotor inlet flow field is weaken as its distance becomes far from rotor leading edge.

Acknowledgement

Finally the authors wish to thank Messrs. T. Nakano, H. Sugimachi, S. Kumamoto, T. Tsutsumi, Y. Takada, and M. Nishimura for assistance in the experimental works.

References

Garnier, V. H., Epstein, A. H., and Greitzer, E. M., 1991, "Rotating Waves as a Stall Inception Indication in Axial Compressors," *ASME Journal of Turbomachinery*, Vol. 113, pp. 290~301.

Moore F. K., and Greitzer E. M., 1986, "A Theory of Post-Stall Transients in Axial Compressor Systems: Part Ⅰ, Ⅱ," *ASME Journal of Engineering for Gas Turbine and Power*, Vol. 108, pp. 68~76, pp. 231~239.

Poensgen C. A., Gallus H. E., 1996, "Rotating Stall in a Single-Stage Axial Flow Compressor," *ASME Journal of Turbomachinery*, Vol. 118, pp. 189~196.

Saxer-Felice H. M., Saxer A., Inderbitzin A., and Gyarmathy G., 1998, "Prediction and Measurement of Rotating Stall Cells in an Axial Compressor," *ASME Paper*, 98-GT-227.

McDougall, N. M., Cumpsty, N. A., and Hynes, T. P., 1990, "Stall Inception in Axial Compressors," *ASME Journal of Turbomachinery*, Vol. 112, pp. 116~125.

Mathioudakis, K., and Breugelmans, F. A. E., 1985, "Development of Small Rotating Stall in a Single Axial Compressor," *ASME Paper*, No. 85-GT-227.

Inoue M., Kuroumaru M., Furukawa M., Tanino T., and Maeda S., "Making of Stall Cell Animation by Double-Phase-Locked Averaging Method," *Turbomachinery*, 27-8, pp. 502~508. (in Japanese)

Inoue M., Kuroumaru M., Tanino T., Furukawa M., "Propagation of Multiple Short-Length-Scale Stall Cells in an Axial Compressor Rotor," *ASME Journal of Turbomachinery*, Vol. 122, pp. 45~54.

Kaneko K., Setoguchi T. and Muraoka A., 1993, "Internal Flow of High Specific Speed Diagonal Flow Fan in Low Flow Range," *Proc. of the 4th Asian Int.* Conf. on Fluid Machinery, pp. 83~88.

Kaneko K., Muraoka A., Shiraishi K., and Setoguchi T., 1995, "Unsteady Flow in Diagonal Flow Fan in Low Flow Range," *Proc. of the 6th Asian Congress of Fluid Mechanics*, Vol. 2, pp. 1488~1491.

Kaneko K., Shiomi N., Muraoka A., and Setoguchi T., 1997, "Internal Flow of High Specific Speed Diagonal Flow Fan with Rotating Stall," *Proc. of the 5th Asian Int. Conf. on Fluid*

Machinery, pp. 795~802.

Shiomi N., Kaneko K., and Setoguchi T., 2000, "Internal Flow of High Specific-Speed Diagonal Flow Fan with Rotating Stall (Behavior of Stall Cell)," *Proc. of the 6th Asian Int. Conf. of Fluid Machinery*, pp. 19~24.